

Surface-related capacitance of microporous carbons in aqueous and organic electrolytes

T.A. Centeno ^a, F. Stoeckli ^{b,1}

^a *Instituto Nacional del Carbón-CSIC, Apartado 73. E-33080 Oviedo, Spain*

^b *Department of Physics, Université de Neuchâtel. Rue Emile Argand 11, CH-2009 Neuchâtel, Switzerland*

Abstract

This paper examines the surface-related capacitance C/S of carbons with average micropore widths between 0.73 and 1.80 nm, using 1-2M H₂SO₄, 6M KOH and 1M (C₂H₅)₄NBF₄ in acetonitrile as electrolytes. Following corrections for pseudocapacitance effects for the aqueous electrolytes and the use of an average surface area suggested by independent techniques, different from the BET area, it appears that C/S is practically independent of the micropore width. The analysis of the data with the help of recent models suggests that the dielectric constants ϵ_r of the different electrolytes may decrease with the pore size. It is surprising that the coexistence of two sets of values for the surface area of microporous carbons and its consequence on C/S have not received more attention in the past.

¹ Corresponding author. Tel.: +41 32 7182425; Fax: +41 32 7182511.

E-mail address: fritz.stoeckli@unine.ch (F. Stoeckli)

Keywords: Electrochemical capacitor; Carbon; Microporosity; Surface functionalities; Dielectric constant.

1. Introduction

The distribution of K^+ ions and water in electrified slit-shaped carbon micropores of accessible width $2b$ between 0.936 to 1.47 nm has recently been investigated by Feng *et al.* [1], using molecular dynamics simulations. This interesting paper, leads to the so-called 'sandwich capacitance model', which can probably be extended to other aqueous electrolytes. The surface-related capacitance ($F\ m^{-2}$) of this type of carbon-based supercapacitor is given by

$$C/2A = \epsilon_r \epsilon_0 / (b - a_0) \quad (1)$$

C is the gravimetric capacitance ($F\ g^{-1}$), $2A$ is the total surface area S of the carbon ($m^2\ g^{-1}$) and a_0 is the radius of the ion (K^+ for the negative electrode).

This expression is complementary to the equations proposed earlier by Huang *et al.* [2,3] for cylindrical mesopores and micropores. In the case of mesopores of radius b , the ions can form a double layer of thickness d on the walls and

$$C/A = \epsilon_r \epsilon_0 / b \ln[b/(b-d)] \quad (2)$$

On the other hand, in cylindrical micropores the reduced width no longer allows the formation of a double layer and it is assumed that the ion of radius a_0 occupies a central position, along the axis of the pore. This leads to

$$C/A = \epsilon_r \epsilon_0 / b \ln(b/a_0) \quad (3)$$

Equations (2) and (3) have been used to analyze the experimental data obtained for aqueous and organic electrolytes [2,3], whereas the more recent Eqn. (1) has only been used, so far, to examine the case of the 6M KOH electrolyte with a series of five carbons (Table 1) [1]. It should also be pointed out that the data for the surface-related capacitance C/S was based essentially on the BET surface area, which is known to be unreliable in the case of nanoporous carbons [4-6]. Moreover, for classical aqueous electrolytes such as H₂SO₄ and KOH, the experimental values of C (F g⁻¹) also contain contributions from pseudocapacitance effects which can be relatively important. They have been examined by different authors [7-14] and depend on the heteroatoms, such as nitrogen and oxygen, present in surface complexes or in the solid. Therefore, appropriate corrections must be applied, since the above models do not consider these effects. On the other hand, their influence is very small in the case of the organic electrolyte (C₂H₅)₄NBF₄ in acetonitrile (TEABF₄/AN) [10,11,13].

The determination of the surface area accessible to the ions of the electrolyte is an important factor in the assessment of C/S and it is surprising that a majority of authors use the BET-based area S_{BET}, in spite of its shortcomings. It has been shown recently [6] that a set of coherent surface areas can be obtained for nanoporous carbons by using independent techniques such as Kaneko's comparison plot based on nitrogen adsorbed at 77 K [15], the adsorption of

phenol from aqueous solutions [16], the Dubinin equation [17,18] and the NLDFT method [19]. The first two techniques are model-independent, whereas the latter assume locally slit-shaped micropores. These areas are usually in good agreement for pores below 1.5-1.8 nm, which suggests that the micropores are predominantly slit-shaped. This is also indicated by the good agreement between the pore size distributions obtained by modeling and by the adsorption of vapours and liquids with molecular dimensions between 0.4 and 1.5 nm [18]. On the other hand, the model of cylindrical micropores assumed by Huang et al. [2,3] is less likely. It also leads to much higher surface areas and to contradictions with the adsorption of molecular probes. This implies that the use of Eqn. (3) in the case of microporous carbons may be problematic, as opposed to mesoporous carbons.

One may consider that the average of the different areas obtained by the techniques mentioned above, S_{av} , is a reliable assessment of the surface area probed by small molecules in typical microporous carbons. (However, it should be pointed out that in a few cases S_{NLDFT} , the area based on NLDFT, shows unexplained deviations from the other three areas). As shown in [6] and illustrated by a few examples in Table 1, the different techniques agree usually within a few percent, but they often diverge from S_{BET} . However, it should be pointed out that in a few cases S_{NLDFT} , the area based on NLDFT, also shows unexplained deviations from the other determinations. This justifies the combination of different techniques, in order to get a good estimate of the surface area, rather than to rely on a single determination.

The study of 42 carbons with average pore sizes between 0.6 and 1.7 nm [6] suggested that

$$S_{\text{BET}} = S_{\text{av}}(1.19 \pm 0.03) L_o \quad (4)$$

where L_o is the average micropore width (Note that all pore widths used in the present study refer to the accessible width, as confirmed independently by pore size distributions based on the adsorption of probes with different molecular dimensions and electron microscopy [18]).

Below 0.9 nm S_{BET} underrates the more likely area S_{av} and above 0.9 nm it gradually overrates it. On average, the ratio $S_{\text{BET}}/S_{\text{av}}$ nearly doubles between 0.9 and 1.6 nm and this difference has a strong influence on surface-related properties of microporous carbons. On the other hand, S_{av} and S_{BET} become similar in mesopores above 4 to 5 nm.

A closer analysis also shows that for a large number of carbons with an external surface area S_e and a micropore volume W_o (or V_{mi}), the ratio $(S_{\text{BET}} - S_e)/W_o$ is around $2500 \text{ m}^2 \text{ cm}^{-3}$ [6] (Typical values are shown in Table 1). It is close to the monolayer equivalent of the nitrogen filling the pore (2814 m^2 per cm^3 for the free liquid at 77 K) and suggests that $S_{\text{BET}} - S_e$ does not represent the real surface area of the micropores, except for pores of 0.8 to 0.9 nm, which can accommodate two layers of nitrogen.

There also exists another contradiction as far as the micropore width is concerned when S_{BET} is used: Many authors who base their study on S_{BET} also

use the average pore width L_o determined either by NLDFT or Dubinin's theory. Both widths are based on the model of slit-shaped micropores and L_o may cover the entire range of microporosity (0.4 to 2 nm). However, if one uses S_{BET} , the average width corresponding to these pores is given by the simple geometrical relation $L_{o\ BET} \text{ (nm)} = 2000 W_o(\text{cm}^3 \text{ g}^{-1}) / (S_{BET} - S_e)(\text{m}^2 \text{ g}^{-1})$. For most carbons this leads a value around $2000/2500 \sim 0.8$ nm. This result is in clear contradiction with $L_{o\ NLDFT}$ or $L_{o\ DUBININ}$ used simultaneously to study the variation of surface-related properties such as C/S_{BET} with the average pore width. Since W_o is a reliable quantity, this paradox clearly illustrates a problem related to S_{BET} , but it has not been addressed to date.

It is surprising that the coexistence of two sets of data for the surface area of microporous carbons, S_{av} and S_{BET} , has not received more attention, because their use in the conversion of gravimetric capacitances C (F g^{-1}) to surface-related capacitances C/S (F m^{-2}) leads to widely different pictures. This aspect and its consequences justify to a large extent the present study which examines the case of the 1-2M H_2SO_4 and 6M KOH aqueous electrolytes (where pseudocapacitance effects must also be considered), as well as the organic medium 1M TEABF_4/AN . Basically, we limit ourselves to microporous carbons with average pore widths L_o between 0.7 and 1.8 nm, where the most important differences appear between the results based on either S_{av} or S_{BET} .

It will be shown that the corrected values of C/S are practically independent of the pore size, which suggests that the dielectric constant may decrease as the pore size decreases.

2. Experimental

The study is based on 18 well characterized carbons (Table 2) for which [CO], the amount of CO released in TPD (thermally programmed desorption), has been determined [8]. Furthermore, 5 porous carbons N0-N4 used previously by us [11] were also included, since their data for the 6M KOH electrolyte was used by Feng *et al.* to validate Eqn. (1) [1]. Sample N0 corresponds to the commercial activated carbon, Norit ® SX2 POCH-Poland. Carbons N1 to N4 resulted from the treatment of N0 by KOH to weight losses around 30 and 50% [11]. For this series of carbons no TPD data was available, but the content of nitrogen and oxygen atoms relative to carbon, (N+O)/C (%) is known [11]. As shown by different authors [9,11,12], this parameter can also be used to estimate pseudocapacitance effects.

The solids have been characterized by different and converging techniques, such as N₂ adsorption at 77 K (*Micromeritics ASAP 2010*) and immersion calorimetry at 293 K. The average surface areas S_{av} (Tables 1 and 2) were determined for each carbon individually from the nitrogen comparison plot, Dubinin's theory and the adsorption of phenol from aqueous solutions monitored by immersion calorimetry [6]. As illustrated by the examples of Table 1, these averages are relatively accurate (standard deviations of a few percent only). With the exception of carbons AZ46-0, XC-72 and N-125, the external surface area S_e represents 1 to 5 per cent of S_{av} (and even less for S_{BET}), which corresponds to a small meso- and macroporosity.

The electrochemical measurements were carried out in two-electrode capacitors with carbon pellets of comparable mass, separated by a glassy fibrous material [8,11]. 1-2M H₂SO₄, 6M KOH aqueous solutions and 1M (C₂H₅)₄NBF₄ in acetonitrile were used as electrolytes. The capacitance values C (expressed per active mass of a single electrode) were estimated by galvanostatic charging-discharging cycles at 50 mA g⁻¹. Obviously, it is an average since the capacitances of the positive and negative electrodes can be different [14].

Tables 1 and 2 give the main structural and electrochemical properties of the different carbons.

3. Results and discussion

3.1. Specific capacitance C/S of carbons in 2M H₂SO₄ and 1M TEABF₄/AN

Different authors [7,8,10,11,13] have suggested that pseudocapacitance effects are related to surface groups which lead to the desorption of CO in TPD and, as illustrated by Fig. 1, the plot of C(2M H₂SO₄)/S_{av} versus [CO]/S_{av} for the group of 18 carbons of Table 2 leads to

$$C(2M H_2SO_4)/S_{av} (F m^{-2}) = (0.104 \pm 0.007) + (51 \pm 6) [CO]/S_{av} \quad (5)$$

(correlation coefficient of 0.890).

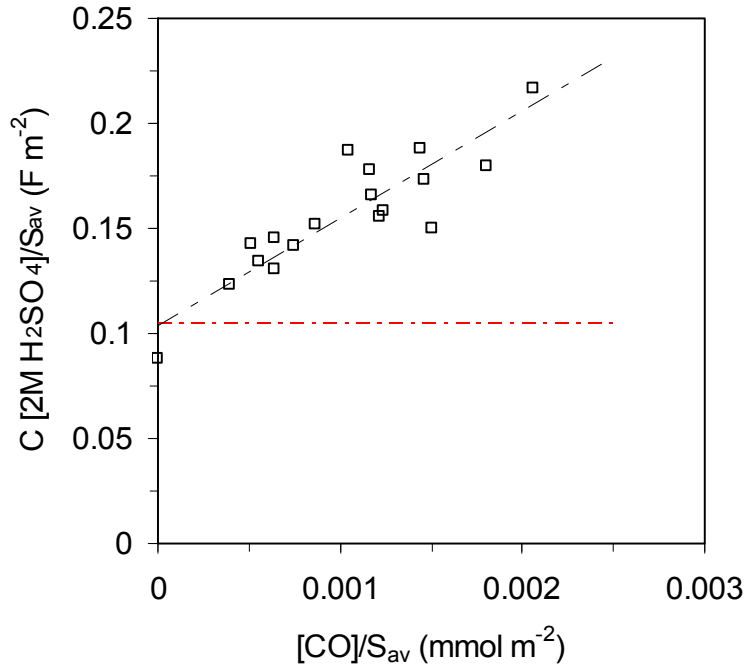


Fig. 1. Variation of the surface-related capacitance $C(2M H_2SO_4)/S_{av}$ with the amount of CO produced in TPD per m^2 of carbon, $[CO]/S_{av}$ (Table 2). The horizontal line corresponds to the average $C(2M H_2SO_4)/S_{av} = 0.104 Fm^{-2}$ suggested by Eqn. (5).

Eqn. (5) suggests a pseudocapacitance effect of approximately 51 F per mmol of CO released in TPD per gramme of carbon. It is similar to the value obtained in an earlier study [8] limited to the total surface area derived from the Dubinin theory, but in good agreement with S_{av} ,

$$C/S_{tot} (F m^{-2}) = (0.081 \pm 0.007) + (63 \pm 5) [CO]/S_{tot} \quad (6)$$

If one uses S_{BET} instead of S_{av} , Eqn. (5) becomes

$$C (2M H_2SO_4)/S_{BET} (F m^{-2}) = (0.072 \pm 0.017) + (62 \pm 12) [CO]/S_{BET} \quad (7)$$

with a correlation coefficient of only 0.600.

An earlier study of Bleda-Martínez et al. [7] based on S_{BET} and examining the capacitance of 1M H_2SO_4 in a variety of activated carbons had led to approximately $0.045 F m^{-2}$ and 75 F per mmol $CO g^{-1}$. Values around 50-80 F per mmol of $CO g^{-1}$ reflect certain types of surface complexes found in typical activated carbons based on lignocellulosic precursors or on natural carbons. On the other hand, lower values were found with certain fibers, as reported recently by Barranco *et al.* [13]. These authors showed that for 2M H_2SO_4 , 1M KOH and 1M TEABF₄/AN the capacitance of amorphous carbon fibers can be fitted to

$$C (F g^{-1}) = A \cdot S_{BET} + B [CO] \quad (8)$$

Parameters A and B are respectively $0.10 \pm 0.02 F m^{-2}$ and $42 \pm 8 F$ per mmol $CO g^{-1}(H_2SO_4)$; $0.078 \pm 0.006 F m^{-2}$ and $35 \pm 3 F$ per mmol $CO g^{-1}$ (KOH); $0.063 \pm 0.006 F m^{-2}$ and $0 \pm 4 F$ per mmol $CO g^{-1}$ (TEABF₄/AN). The pseudocapacitance effect in 2M H_2SO_4 is smaller for the fibers than for the other types of carbons, as also observed by us for two series of activated fibers giving approximately 25 F per mmol $CO g^{-1}$ (unpublished results).

With the value of 51 F per mmol of $CO g^{-1}$ suggested by Eqn. (5), it is possible to calculate the individual capacitances of the 18 carbons in the absence

of pseudocapacitance effects, $C(2M H_2SO_4)/S_{av}$ -corr. (see Table 2). As illustrated by Fig. 2, they show no trend with the average pore width L_o .

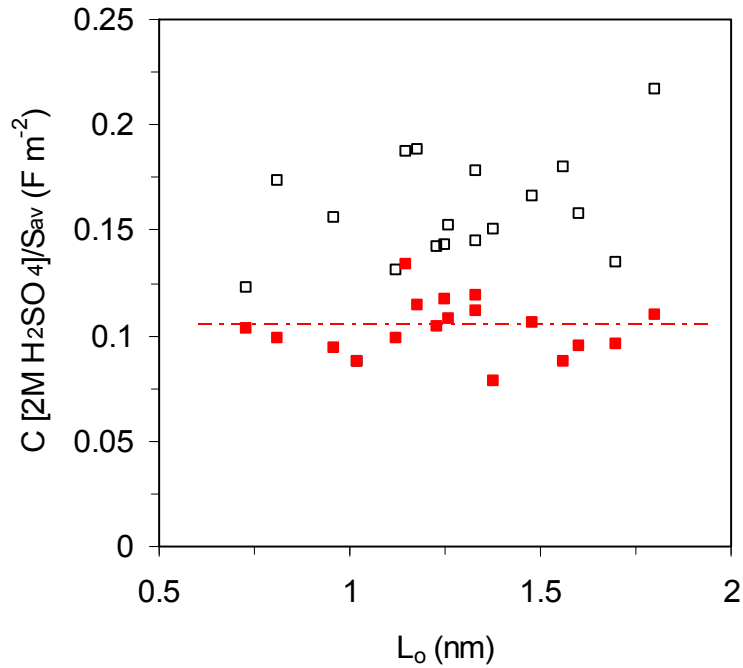


Fig. 2. Comparison of the variation of the initial $C(2M H_2SO_4)/S_{BET}$ (□) and the corrected $C(2M H_2SO_4)/S_{av}$ -corr. (■) capacitances of carbons of Table 2 with their average micropore width L_o . The dotted line corresponds to the average of $0.104 F m^{-2}$ suggested by Eqn. (5).

In the 1M TEABF₄/AN electrolyte, pseudocapacitance effects are much smaller or inexistent and C/S_{av} is practically independent of L_o , whereas C/S_{BET} clearly increases as L_o decreases (see Fig. 3). Lower values of C/S_{av} observed for certain carbons (CMS, XC-72, PC94-11) with L_o near or below 1 nm reflect restricted adsorption of the relatively large $(C_2H_5)_4N^+$ ion (0.68 nm [3]), due to constrictions and/or smaller pores. Consequently, this ion cannot access the

entire area S_{av} suggested by small probes such as nitrogen. This is confirmed by the lower enthalpies of immersion [18] of these carbons into CCl_4 (also 0.68 nm) than into benzene. The latter can probe all pores and in the case of equal accessibility for both liquids, the two enthalpies should be equal. It follows that for carbons CMS, XC-72 and PC94-11 the real values of $C(1M\ TEABF_4/AN)/S$ should be somewhat higher and close to the value of the other carbons (on average around $0.090\ F\ m^{-2}$).

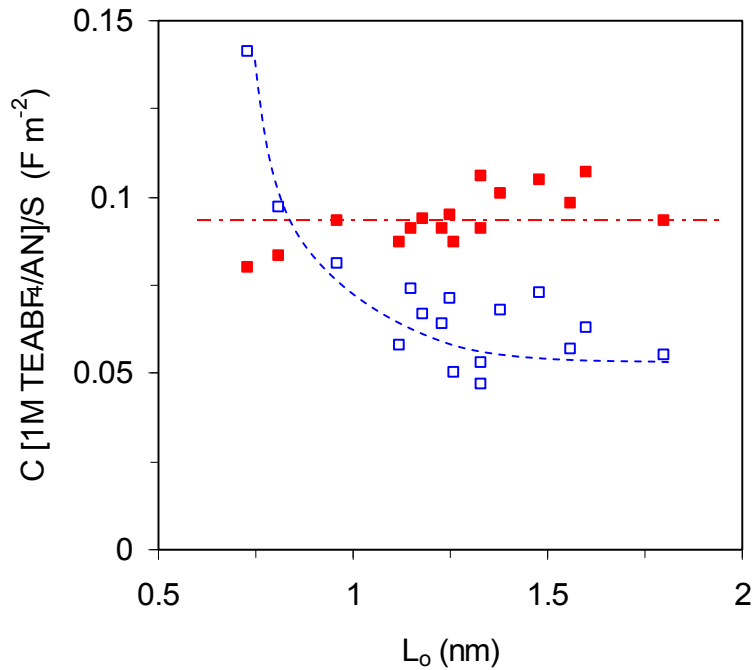


Fig. 3. Variation of the capacitances $C(1M\ TEABF_4/AN)/S_{BET}$ (□) and $C(1M\ TEABF_4/AN)/S_{av}$ (■) of 16 carbons of Table 2 with their average micropore width L_o . The dotted curve shows the trend in (□) and the horizontal dotted line corresponds to the average of (■), $0.095\ F\ m^{-2}$.

The fundamental difference between C/S_{av} and C/S_{BET} reflects the fact that S_{BET} overrates the surface area above 0.9 nm and underestimates it below this value, as suggested by Eqn. (4). This trend also corresponds to the behavior reported for carbide-based carbons (CDCs), suggesting an anomalous increase in C/S_{BET} below 1 to 1.2 nm [21,22].

At this stage it is interesting to mention the recent work of Zhene Feng *et al.* [23] based on eight carbons with micropores and different types of mesopores. These authors showed that a refined analysis of C(TeABF₄/polycarbonate)/S based on S_{NLDFT} (an area usually close to S_{av} [6]), leads to specific capacitances of respectively 0.087, 0.099, and 0.097 F m⁻² in pores below 1 nm, between 1 and 2 nm, and above 2 nm. This would confirm that the surface-related capacitance does not depend on the pore size, as suggested by earlier observations [10, 24].

3.2. Specific capacitances C/S of samples N0-N4 in 1M H₂SO₄, 6M KOH and 1M TEABF₄/AN

For samples N0-N4 of Table 1 no information regarding TPD is available, but following earlier studies [9,11,12], the effect of pseudocapacitance effects can also be assessed by considering the ratio of nitrogen and oxygen relative to carbon, (N+O)/C. Although the pseudocapacitance mechanisms are different, the ratios of the capacitances $C(6M\ KOH)$ and $C(1M\ H_2SO_4)$ measured at 50 mA g⁻¹, are close to (0.97 ± 0.03) and the combination with data for 9 other carbons [8,25,26] with similar ratios suggests the overall correlation

$$C/S_{av} (\text{Fm}^{-2}) = (0.115 \pm 0.004) + (3.6 \pm 0.6)[((\text{O+N})/\text{C}) / S_{av}] \quad (9)$$

valid for both electrolytes. The third term can be used to correct the individual values of the capacitances C/S_{av} of the present series of carbons. For carbons N0-N4 alone, the use of S_{av} and S_{BET} leads respectively to 2 and 3.6 F per % of (N+O) relative to carbon and m^{-2} . This justifies the use of a factor around 3 F per % m^{-2} as a good approximation to correct the data for pseudocapacitance effects. (As shown below, this choice is confirmed by the good agreement found in the case of 1M H_2SO_4 when compared with the values of carbons 1 - 18, Table 2).

As shown in Table 1, the values of $C(6\text{M KOH})/S_{BET}$ and $C(1\text{M H}_2\text{SO}_4)/S_{BET}$ both appear to increase as the pore width L_o decreases from 1.45 to 1.06 nm. However, if one uses S_{av} instead of S_{BET} the trend is practically eliminated, with the exception of the values at 1.06 nm. The latter reflects the much higher fraction of heteroatoms (N+O)/C in sample N0 than in N1 to N4. For the latter samples, which have similar fractions of heteroatoms, the changes between C/S_{BET} and C/S_{av} illustrate the importance of the choice of the surface area. A similar situation is suggested by the analysis of Shi's data [20], giving both S_{NLDFT} and S_{BET} for series of carbons used in the study of C (6M KOH). Shi also pointed out the agreement between S_{NLDFT} and S_{DR} and their divergence with S_{BET} , but this observation seems to have been largely ignored.

Using the correction factor of 3.6 F per %(N+O)/C and m^{-2} suggested by Eqn. (9), one obtains the real surface-related capacitances of carbons in 6M

KOH and 1M H₂SO₄. As seen in Table 1, the trends suggested by the C/S_{BET} values are no longer perceptible for these electrolytes. The values of the corrected capacitances C(1M H₂SO₄)/S_{av}-corr. are similar to those obtained with the series of 18 carbons (Table 2), whereas those of C(6M KOH)/S_{av}-corr. are slightly smaller.

In the case of the 1M TEABF₄/AN electrolyte, the values of C/S_{av} are similar to those obtained for the samples of Table 2.

The absence of a trend in the surface-related capacitance based on S_{av} and following possible corrections for pseudocapacitance effects has consequences which are examined in the following section.

3.3. Comparison with models and possible consequences

Since micropores are locally slit-shaped, the data for 6M KOH electrolyte can be used first as a test case for Eqn. (1). The model of Feng *et al.* [1] suggests that C(6M KOH)/S should increase as the pore width decreases from 1.5 to 0.9 nm. This seems to be the case for the uncorrected experimental data C(6M KOH)/S_{BET} of samples N4-N0, where L_o varies between 1.45 and 1.06. The fit of this data to Eqn. (1) led these authors to the conclusion that $\epsilon_r = 3.33 \pm 0.57$ and $a_o = 0.265 \pm 0.054$ nm [1], which are averages between the corresponding values of the positive and the negative electrodes. However, as shown above, the more likely areas S_{av} alone, as well the subsequent corrections for pseudocapacitance effects, suggest relatively constant surface-related capacitances over the range of microporosity considered here (0.7 to 1.8 nm).

This leads to a completely different picture when examined in the light of Eqn. (1). As the model of Feng *et al.* [1] is certainly realistic, constant values of C/S imply that the change in pore width must be compensated by another change in Eqn. (1). One may consider either (i) an increase in ϵ_r at constant a_o , (ii) an increase in a_o at constant ϵ_r or (iii) a variation of both parameters. In the first case, assuming a constant radius $a_o = 0.138$ nm for the K^+ ion [1] and using C(6M KOH)/ S_{av} -corr., Eqn.(1) suggests that ϵ_r decreases from 7.1 to 4.2 as the average pore size L_o decreases from 1.45 to 1.06 (see Table 1). The second possibility, based on $\epsilon_r = 3.33$ suggests that a_o increases from 0.22 and 0.45 nm and for $\epsilon_r = 6.0$, the values are between 0 and 0.23. These values are somewhat unrealistic and the possibility of a gradual decrease of ϵ_r as the pore size decreases, seems more plausible. Moreover, there is no reason in the derivation of Eqns. (1)-(3) [1-3] that ϵ_r should be constant. Its reduction, implied by a constant C/S, may well reflect the gradual desolvation of the constant number of ions in the pore as the amount of water decreases in the smaller pore.

As seen in Tables 1 and 2, the corrected data for 1M H_2SO_4 , 2M H_2SO_4 and 1M TEABF₄/AN suggests the same pattern for these electrolytes. One may assume that the 'sandwich capacitance model' of Eqn. (1) also applies to these electrolytes.

These examples show the consequence resulting from the use of S_{av} instead of S_{BET} , when gravimetric capacitances are converted to surface-related capacitances and corrected for pseudocapacitance effects where needed.

The hypothesis of a variable dielectric constant suggested by the present approach seems quite plausible in view of the change in ϵ_r reported for the adsorption of water in microporous clays [27,28] and in particular in expanding montmorillonites [29]. Their structure consists of negatively charged layers with Na^+ or Ca^{+2} cations between them, which are solvated by water. This situation is similar to the negative electrode of the 'sandwich capacitance model' (solvated K^+ ion), except that the montmorillonite layers are non-conducting.

In the case of Na- and Ca-bentonites (impure montmorillonites), *in-situ* X-ray measurements of the d_{001} spacing [30] showed that the water uptake begins with successive openings of the interlayer space to 0.27 nm and 0.56 nm corresponding to the complete two- and three dimensional solvations. This is followed by a gradual widening of the slits up to 1.04 nm, where the water uptake is 40% w/w and beyond. Moreover, at all stages the pores are completely filled with water.

As illustrated by Fig. 2 of the paper by Cosenza and Tabbagh [27], the dielectric constants within natural expansive clays and bentonite increase in the range of 5 to 20 with the water uptake, itself directly related to the interlayer spacing. In other words, ϵ_r decreases gradually as the pore width decreases and the amount of water surrounding the Na^+ or Ca^{+2} ions is reduced. It is likely that a similar pattern applies to the relative permittivity ϵ_r of aqueous electrolytes in the slit-shaped micropores of carbons, in particular when the ratio of water molecules to the constant number of ions decreases. Moreover, molecular dynamics simulations carried out by Senapati *et al.* [31] suggest that even the

dielectric constant of pure water confined in nanocavities with diameters between 2.44 and 1.22 nm should be reduced from 71 to 42. This is a further justification for the hypothesis of a gradual decrease of ϵ_r in micropores of decreasing width. However, a contribution cannot be excluded from parameter a_0 which corresponds to the thickness of the double layer d in mesopores pores, but the present study deals exclusively with microporous carbons below 1.8 nm with little mesoporosity.

4. Conclusions

The present study illustrates the importance of the assessment of the surface area of microporous carbons, as well as taking into account corrections for pseudocapacitance effects which are present in the case of aqueous electrolytes such as H_2SO_4 and KOH .

The choice of the surface area used to convert the reliable gravimetric capacitance C ($F g^{-1}$) into a surface-related quantity C/S ($F m^{-2}$) appears to be of fundamental importance. It is therefore surprising that the coexistence of S_{BET} and other surface area determinations, summed up by S_{av} , has not received more attention in view of its consequences. This justifies the closer examination presented here.

The BET technique is known to be unreliable in the case of nanoporous carbons, as confirmed by an IUPAC recommendation [4] and detailed studies [5,6], but S_{BET} is still widely used. It appears that in the case of typical microporous carbons (predominantly locally slit-shaped pores of widths between

0.7 and 1.8 nm), the use of the more plausible surface area S_{av} leads to relatively constant specific capacitances in typical aqueous and organic electrolytes (1-2M H_2SO_4 , 6M KOH and 1M TEABF₄/AN). On the basis of Eqn. (1), which corresponds to a realistic model for slit-shaped micropores, one reaches the conclusion that the dielectric constant ϵ_r may decrease with the pore width. This behaviour is also suggested by analogy with the variation of ϵ_r observed in bentonites, where the water uptake leads to a gradual widening of the interlayer spacing. This system is similar to the negative electrode of the KOH electrode described by Eqn. (1).

References

1. G. Feng, R. Qiao, J. Huang, B.G. Sumpter, V. Meunier, *ACS Nano* 4 (2010) 2382.
2. J. Huang, B.G. Sumpter, V. Meunier, *Angew. Chem.* 47 (2008) 520.
3. J. Huang, B.G. Sumpter, V. Meunier, *Chem. Eur. J.* 14 (2008) 6614.
4. J. Rouquérol, D. Avnir, C. W. Fairbridge, D. H. Everett, J. M. Haynes, N. Pernicone, J. D. F. Ramsay, K. S. W. Sing, K. K. Unger, *Pure Appl. Chem.* 66 (1994) 1739.
5. J. Rouquérol, P. Llewellyn, F. Rouquérol. In: Llewellyn P, Rodriguez-Reinoso F, Rouquérol J, Seaton N, editors. *Studies in Surface Science and Catalysis* 160. Elsevier. Amsterdam 2007. p. 49-56.
6. T.A. Centeno, F. Stoeckli, *Carbon* 48 (2010) 2478.
7. M.J. Bleda-Martínez, J.A. Maciá-Agulló, D. Lozano-Castelló, E. Morallón, D. Cazorla-Amorós, A. Linares-Solano, *Carbon* 43 (2005) 2677.
8. T. A. Centeno, F. Stoeckli, *Electrochim. Acta* 52 (2006) 560.
9. D.W. Wang, F. Li, M. Liu, H.M. Cheng, *New Carbon Materials* 22 (2007) 307.
10. T.A. Centeno, M. Hahn, J.A. Fernández, R. Kötz, F. Stoeckli, *Electrochem. Comm.* 9 (2007) 1242.
11. G. Lota, T.A. Centeno, E. Frackowiak, F. Stoeckli, *Electrochim. Acta* 53 (2008) 2210.
12. E.J. Ra, E. Raymundo-Piñero, Y.H. Lee, F. Béguin, *Carbon* 47 (2009) 2984.
13. V. Barranco, M. A. Lillo-Rodenas, A. Linares-Solano, A. Oya, F. Picó, J. Ibañez, F. Agullo-Rueda, J. M. Amarilla, J. M. Rojo, *J. Phys. Chem. C* 114 (2010) 10302.
14. G. Lota, J. Tyczkowskib, R. Kapicab, K. Lota, E. Frackowiak, *J. Power Sources* 195 (2010) 7535.
15. N. Setoyama, T. Suzuki, K. Kaneko, *Carbon* 36 (1998) 1459.

16. E. Fernández, D. Hugi-Cleary, V. López-Ramón, F. Stoeckli, *Langmuir* 19 (2003) 9719.
17. M.M. Dubinin, *Carbon* 27 (1989) 457.
18. F. Stoeckli, in *Porosity in carbons. Characterization and applications*, (Ed: J. Patrick), Arnold, London, 1995, pp. 67-92.
19. P.I. Ravikovich, A. Vishniakov, R.A.Russo, V. Neimark, *Langmuir* 16 (2000) 2311.
20. H. Shi, *Electrochim. Acta* 41 (1996) 1633.
21. J. Chmiola, G. Yushin, Y. Gogotsi, C. Portet, P. Simon, P.L. Taberna, *Science* 313 (2006) 1760.
22. P. Simon, Y. Gogotsi, *Nat. Mater.* 7 (2008) 845.
23. Z. Feng, R. Xue, X. Shao, *Electrochim. Acta* 55 (2010) 7334.
24. O. Barbieri, M. Hahn, A. Herzog, R. Kötz, *Carbon* 43 (2005) 1303.
25. T.A. Centeno, F. Stoeckli, *J. Power Sources* 154 (2006) 314.
26. A.B. Fuertes, G. Lota, T.A. Centeno, E. Frackowiak, *Electrochim. Acta* 50 (2005) 2799.
27. P. Cosenza, A. Tabbagh, *Appl. Clay Sci.* 26 (2004) 21.
28. V. Saltas, F. Vallianatos, D. Triantis, *J. Non-Cryst. Solids*, 354 (2008) 5533.
29. H. Bidadi, P.A. Schroederer, T. Pinnavaia, *J. Phys. Chem. Solids* 49 (1988) 1435.
30. F. Kraehenbuehl, F. Stoeckli, F. Brunner, G. Kahr, A. Müller-Vonmoos, *Clay Miner.* 22 (1987) 1.
31. S. Senapati, A. Chandra, *J. Phys. Chem. B* 105 (2001) 5106.

Table 1. Structural and electrochemical properties of carbons N0-N4.

Carbon		N0	N1	N2	N3	N4
L_o (nm)		1.06	1.09	1.34	1.36	1.45
S_e ($m^2 g^{-1}$)		17	23	30	64	50
S_{av} ($m^2 g^{-1}$)		657 ± 34	1310 ± 49	1419 ± 42	1425 ± 45	1536 ± 56
S_{BET} ($m^2 g^{-1}$)		835	1901	2400	2522	2800
$(S_{BET}-S_e)/W_o$ ($m^2 cm^{-3}$)		2337	2504	2604	2560	2670
(O+N)/C content (% wt.)		8.80	4.11	4.40	4.30	4.11
6M KOH	C/S_{BET} ($F m^{-2}$)	0.113	0.083	0.070	0.075	0.065
	C/S_{av} ($F m^{-2}$)	0.143	0.120	0.118	0.133	0.118
	C/S_{av} corrected ($F m^{-2}$)	0.095	0.109	0.107	0.122	0.108
	ϵ_r Eqn. (1) ($a_o = 0.138$ nm)	4.2	5.0	6.4	7.5	7.1
1M H_2SO_4	C/S_{BET} ($F m^{-2}$)	0.126	0.079	0.071	0.072	0.071
	C/S_{av} corrected ($F m^{-2}$)	0.112	0.105	0.111	0.117	0.118
1M TEABF ₄ /AN	C/S_{BET} ($F m^{-2}$)	0.055	0.063	0.052	0.055	0.052
	C/S_{av} ($F m^{-2}$)	0.070	0.092	0.087	0.098	0.094

Table 2. Structural and electrochemical characteristics of the group of 18 carbons.

Carbon	Lo (nm)	[CO] (mmol g ⁻¹)	S _{BET} (m ² g ⁻¹)	S _{av} (m ² g ⁻¹)	2M H ₂ SO ₄				1M (C ₂ H ₅) ₄ NBF ₄ /AN		
					C (Fg ⁻¹)	C/S _{BET} (Fm ⁻²)	C/S _{av} (Fm ⁻²)	C/S _{av-corr.} [eqn.5] (Fm ⁻²)	C (Fg ⁻¹)	C/S _{BET} (Fm ⁻²)	C/S _{av} (Fm ⁻²)
RM1	0.73	0.43	619	1086	139	0.224	0.123	0.103	87	0.141	0.080
CMS	0.81	0.97	567	665	115	0.203	0.173	0.099	55	0.097	0.083
AZ46-0	0.96	0.98	914	808	126	0.138	0.156	0.094	75	0.082	0.093
XC-72	1.02	0.001	250	250	22	0.088	0.088	0.088	15.8	0.063	-
PC94-11	1.12	0.66	1553	1038	136	0.088	0.131	0.099	90	0.058	0.087
DCG-5	1.15	0.942	1121	903	169	0.151	0.187	0.134	82.5	0.074	0.091
PC94-11ox	1.18	1.2	1165	830	156	0.134	0.188	0.114	78	0.067	0.094
M1-R	1.23	0.82	1555	1095	156	0.100	0.142	0.104	100	0.064	0.091
M1-R (PM)	1.25	0.56	1454	1089	156	0.107	0.143	0.117	103	0.071	0.095
U02-ox	1.26	0.58	1166	670	102	0.087	0.152	0.108	58.2	0.050	0.087
M-30	1.33	1.33	2298	1145	204	0.089	0.178	0.119	121	0.053	0.106
SUPRA-50	1.33	0.67	2013	1049	152	0.076	0.145	0.112	95.6	0.047	0.091
KF-1500	1.38	1.5	1568	1063	159	0.101	0.150	0.078	107	0.068	0.101
F02	1.48	1.0	1223	849	141	0.115	0.166	0.106	89	0.073	0.105
U03	1.56	1.22	1172	676	122	0.104	0.180	0.088	66.5	0.057	0.098
N-125	1.60	0.96	1317	774	122	0.093	0.158	0.095	83	0.063	0.107
PC-92-2	1.70	0.81	1451	1080	145	0.100	0.134	0.096	-	-	-
U03-ox.	1.80	1.42	1166	690	150	0.129	0.217	0.112	64.5	0.055	0.093

